Supporting the Design of On-Site Infiltration Systems: From a Hydrological Model to a Web App to Meet Pluriannual Stormwater Volume Reduction Targets

Jérémie Sage, Emmanuel Berthier, Marie-Christine Gromaire, Ghassan Chebbo

Jérémie Sage, Emmanuel Berthier, Marie-Christine Gromaire, Ghassan Chebbo (2024). Supporting the Design of On-Site Infiltration Systems: From a Hydrological Model to a Web App to Meet Pluriannual Stormwater Volume Reduction Targets, Journal of Hydrologic Engineering, Volume 29, Issue 3

The final publication is available at ASCE via https://doi.org/10.1061/JHYEFF.HEENG-6092

Supporting the design of on-site infiltration systems: from a hydrological model to a web-app to meet pluriannual stormwater volume reduction targets

Jérémie Sage[1], Emmanuel Berthier[2], Marie-Christine Gromaire[3], Ghassan Chebbo[4]

[1]Cerema, Equipe TEAM, 12 Rue Léon Teisserenc de Bort, 78190 Trappes, France ; jeremie.sage@cerema.fr

[2]Cerema, Equipe TEAM, 12 Rue Léon Teisserenc de Bort, 78190 Trappes, France ; emmanuel.berthier@cerema.fr

[3]Leesu, Ecole des Ponts, Université Paris Est Créteil, F 77455 Marne-la-Vallée, France, marie-christine.gromaire@enpc.fr

[4]Leesu, Ecole des Ponts, Université Paris Est Créteil, F 77455 Marne-la-Vallée, France, ghassan.chebbo@enpc.fr

Abstract

Infiltration-based sustainable urban drainage systems (i-SUDS) often turn out to be simple and effective solutions for on-site runoff and pollution control. Their ability to limit the discharge to sewer networks or receiving waters can be broadly assessed in terms of (pluri)annual stormwater volume reduction. Although accepted as a relevant efficiency metric, this long-term volume reduction does not integrate well in design practices that have traditionally relied on event-based approaches. This article introduces a modelling framework, involving a hydrological model and machine-learning emulation, from which a web-app was developed to allow practitioners to investigate the relation between i-SUDS design and pluriannual volume reduction efficiencies. The theoretical basis for modelling and a description of the web-app are first provided. A diagnosis of the hydrological model is then conducted. The uncertainty caused by model parameters that do not directly relate to i-SUDS design is evaluated through a sensitivity analysis performed over multiple design scenarios. The latter is found to be highly variable and potentially significant, thereby justifying its explicit consideration in the web-app. As part of this diagnosis, the impact of a shallow groundwater or a low-permeability layer on simulated volume reduction efficiencies is later evaluated to clarify the validity domain of the model. Practical recommendations on the minimum distance to shallow groundwater or low permeability layer, for the rainfall conditions considered in the web-app, are given as a function of project size and the permeability of the soil media. The applicability of the web-app is later illustrated from a selection of outputs. Its outcomes are finally compared to those of a simple design rule based on the combination permanent storage (as a rainfall depths) and drawdown duration targets. Results confirm the inability of such simple design rules to fully capture pluriannual volume reduction efficiency and point out the risk of oversizing i-SUDS.

Practical applications

Stormwater infiltration in small vegetated systems can effectively reduce runoff and pollutant discharge to surface waters. A well-accepted performance objective for such systems is to achieve a significant reduction of the rainfall volume at the annual scale. Integrating (pluri)annual volume reduction targets in design practices however remains difficult as they do not accommodate well with the back-of-the-napkin, event-based, calculations traditionally used by the stormwater profession. This paper introduces a web-app that allows practitioners to easily investigate the relation between the design characteristics of infiltration-based solutions and pluriannual volume reduction efficiencies. The approach shows how machine-learning can be used to replicate at low computational cost the outputs of specialized hydrological models and be incorporated in larger-audience tools. Through an analysis of the validity domain of the app, the study also points out the potential reduction of efficiency that may result from the presence of a shallow groundwater or a low-permeability layer, an aspect often overlooked in the design of infiltration-based systems. The applicability of the app is illustrated from different usage situations. The relevance of the proposed approach is finally demonstrated through a comparison to a simpler, event-based design method, which proves unable to adequately capture pluriannual volume reduction efficiency.

1 Introduction

1.1 Context and objectives

Sustainable Urban Drainage Systems (SUDS) have progressively emerged as an alternative (or complement) to conventional pipe-based stormwater management infrastructure (Butler et al. 2018; Fletcher et al. 2014). Among the numerous solutions that fall within the SUDS concept, systems in which water is infiltrated at the soil surface (i-SUDS) are of particular interest due to their simplicity and ability to retain runoff on-site, thereby providing local pollution control and also preventing combined sewer overflow or cross-contamination in stormwater networks (Bressy et al. 2014). I-SUDS often consist in relatively simple decentralized, pervious and vegetated solutions that can easily be implemented within urban environments. Disseminated through the city, they also offer perspective to address other environmental issues such as biodiversity loss, temperature rises…(Zhang and Chui 2019).

Because frequent rain events usually represent a large fraction of the annual stormwater volume, the efficiency of (i-)SUDS for runoff and pollution control largely depends on their ability to prevent discharge to sewer systems during such events (Bressy et al. 2014). Stormwater management guidelines have hence gradually evolved to incorporate annual runoff reduction targets or no-discharge criteria for small storms (Nie et al. 2020; Qi et al. 2020; Sage et al. 2015a; US-EPA

2016). Demonstrating compliance with such targets is however not straightforward. Indeed, traditional design-storm methods, still widely used in the urban drainage profession, cannot directly address long-period volume reduction objectives and tend to be less relevant for frequent rain events due to the potentially significant influence of initial moisture conditions (Traver and Ebrahimian 2017).A common expedient is the introduction of permanent storage (i.e., retention volume) targets associated with drawdown requirements as surrogates for annual volume (or sometimes pollutant load) reduction targets (Sage et al. 2015a; US-EPA 2016). In Paris region (Ile-de-France) for example, providing storage for the runoff associated with an 8 to 10 mm rain event and recovering this capacity within 24h without discharge to the sewer system is often assumed to ensure an 80% reduction of the annual rainfall volume (DRIEE 2020, additional references and explanations on this design rule are provided as supplementary material in S1). While such simple static and standardized approaches may sometimes be reasonable, they suffer from several limitations. First, the determination of a permanent storage target (for a given pluriannual volume reduction objective) usually involves a statistical rainfall analysis in which it is necessary to introduce an event-separation criteria (or at least a calculation time-frame) that may arbitrarily affect the outcome of the analysis (Sage et al. 2015a). Secondly, the use of a fixed daily or event-based volume reduction target is not consistent with the variability of surface storage, soil moisture conditions and hydrologic losses at this time scale (Wang 2019). Optimizing the performance of i-SUDS therefore requires adapting design approaches to capture this variability. From a more general perspective, it is also desirable to facilitate the understanding of the impact of design parameters and local soil conditions on the functioning and performance of these systems. To achieve that, preference should be given to methods or tools relying on continuous simulation (Traver and Ebrahimian 2017).

The objective of this article is to introduce a framework (Oasis) consisting of a hydrological model (Oasis-model), a set of neural network emulators (NN) and web-app (Oasis-app) developed to allow practitioners to investigate the relation between the design of on-site stormwater infiltration systems and long-period volume reduction efficiencies “at the site scale” based on continuous simulation. After a brief overview of existing design tools, the theoretical basis for modelling and a description of the web-app are provided. A diagnosis of the hydrological model is then conducted to evaluate i) how uncertain parameters may affect model outputs and ii) for which soil and sub-soil conditions the model may reasonably be applied. The applicability of the web-app later is illustrated from a selection of outputs. Its relevance as an alternative to static design approaches is finally demonstrated from an analysis conducted over a large number of i-SUDS design scenarios.

1.2 Contribution over existing approaches

Numerous tools have been developed to assist practitioners in the implementation of SUDS. These tools can address a variety of issues such as SUDS selection, design or location and involve different scales of applications or levels of complexity (Ferrans et al. 2022). This section solely focuses on those dedicated to the design or performance assessment of SUDS at the site-scale. The aim is to give an overview of existing solutions and to point out some of their key features so as to later clarify the positioning of the modeling framework introduced in this article.

Summaries of current design tools can be found in recent research articles (Kaykhosravi et al. 2018; Shojaeizadeh et al. 2019) or stormwater management manuals (MPCA 2022). These tools can be classified according to their ease-of-use (Shojaeizadeh et al. 2019), with a gradient between specialized computational models, that require a degree of expertise for input preparation or data processing (Beck et al. 2017), and "calculators" that are more specifically intended for practitioners and routine design operations (e.g. identifying possible design configurations for a given stormwater management goal; assessing the hydrological performance of an existing device….). Model belonging to the first category such as SWMM (Rossman 2015), can typically be applied across different spatial scales and to a broad range of problems, from individual SUDS design to multicriteria optimization of SUDS types and location (Ferrans et al. 2022). By contrast, "calculators", such as those cited in Shojaeizadeh et al. (2019) are mostly dedicated to the site-scale. The latter, which sometimes consist in simple spreadsheets, tend to be less documented than the former, which may be used for research purposes.

Another important characteristic is the time scale at which underlying hydrological models operate, with either event-based approaches or continuous simulations (Ferrans et al. 2022). Among "calculators", only a limited number of (recent) tools actually involve continuous modeling. Others, such as MIDS (MPCA 2022) in the US or Parapluie in France (Chocat and Salmoun 2019), rely on design-storm approaches. Examples of calculators involving continuous simulation include EPA's National Stormwater Calculator (SWC) (Rossman and Bernagros 2019), i-DSTss (Shojaeizadeh et al. 2019) and the California Phase II LID Sizing Tool (CA-LID-ST) (CSU 2019). For such tools, results may be generated by performing the simulations in "real time" (i.e., at the user's request) or retrieved from pre-calculated data. In the two first examples, calculations are performed directly (with the SWMM engine or a similar model, resp.) whereas in the third one pre-calculated sizing curves are used to link SUDS design and performance.

Design tools generally allow considering a variety of SUDS type. Those relying on "real time" calculations, offer a large flexibility in the description of the facility, just as the hydrological models they rely on. Conversely, the use of "pre-calculated" outputs involves some simplifications in the description of the facility. For instance, in the CA-LID-ST, the main design parameter is the area of the facility, and the user only has limited control over other design parameters.

Most “calculators” are simple performance assessment tools which generate a limited number of performance metrics from user-specified inputs regarding SUDS design and site conditions. As such, they often do not provide detailed statistics regarding SUDS functioning, a typical feature of more specialized models. A notable exception is SWC (Rossman and Bernagros 2019) which relies on “real time” calculations with the SWMM engine. Another relatively rare feature of “calculators” is the ability to identify optimal SUDS design for a given objective (Shojaeizadeh et al. 2019). When the tool directly relies on long-period calculations, this optimization is generally not implemented (as it can hardly be performed within a reasonable time) (Ferrans et al. 2022). The use of pre-calculated outputs however allows optimization through a limited number of design parameters. In CA-LID-ST, it is for example possible to estimate the area needed to reach volume reduction targets under specific SUDS design conditions (fixed maximum ponding depth, soil media thickness composition…) (CSU 2019). Similarly, most “calculators” mentioned above do not allow visualizing the effect of design parameters on SUDS performance through graphs (although this feature is actually included in i-DSTss, it is limited to a single SUDS area parameter and its applicability for long-period simulation is questionable). Finally, most design tools do not incorporate any kind of uncertainty assessment and simply display single-value outputs. It is however worth noting that EPA’s National Stormwater Calculator provides an option to test and compare different climate change scenarios (Rossman and Bernagros 2019).

As a summary, many of current SUDS design calculators are still based on static or design-storm approaches. Some innovative tools involving continuous modelling were recently introduced, mainly in the US. These tools either rely on real-time simulations or pre-calculated outputs to assess the performance of a variety of SUDS. Both attitudes have their advantages and disadvantages. The Oasis-app, presented in this article, involves a different approach based on hydrological model emulation. The latter allows overcoming some limitations of the above-mentioned methods. It also allows including non-standard features such as a (yet elementary) uncertainty assessment on calculated outputs, visualization of the effect of design parameters based on graphs, design optimization for user-specified volume reduction targets and calculation of various statistics regarding SUDS functioning.

2 Material and methods

The modeling framework is first introduced, giving the main equations of the hydrological model, the method for NN-emulation, and the operating principles of the web-app. The testing stage, consisting of a sensitivity analysis and an evaluation of the validity domain of the hydrological model (and thus the web-app) regarding underground conditions, is

then presented. The approach adopted to demonstrate the applicability of the web-app, and for the most part, its relevance over static design approaches is finally described. These different steps are summarized in Figure 1.

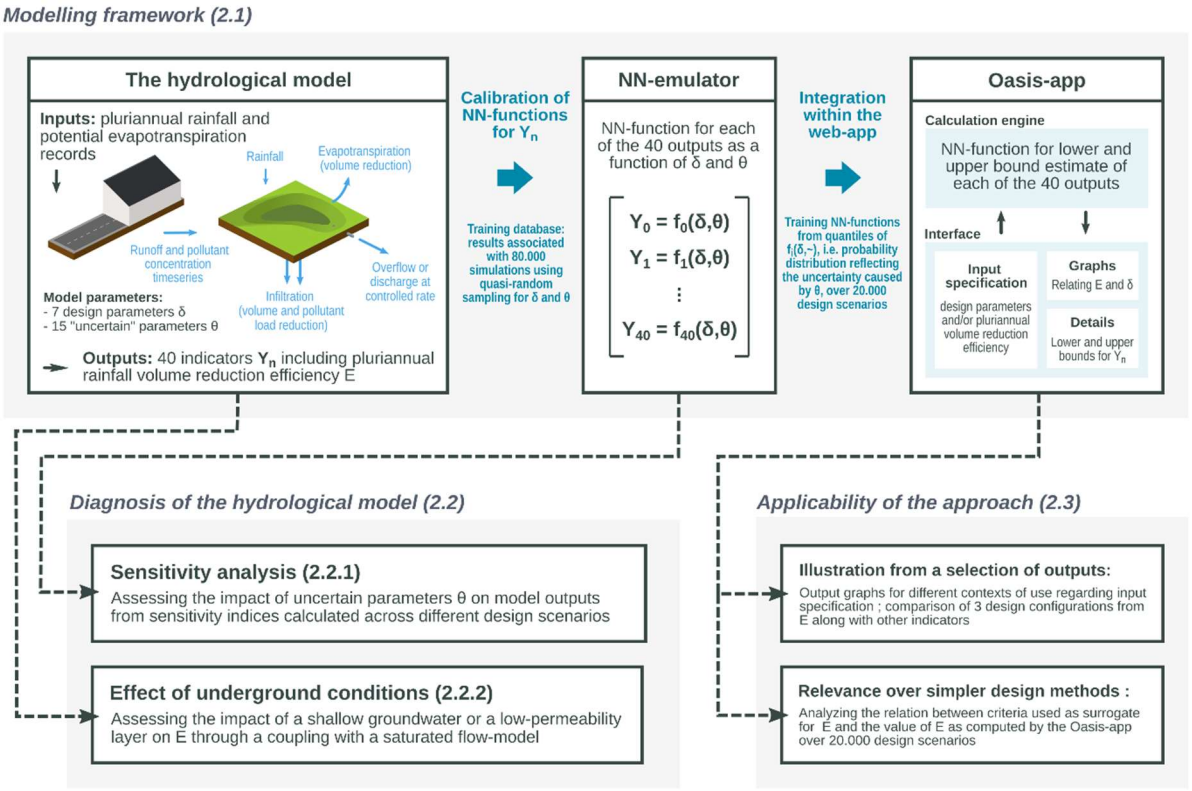

Figure 1 – Linking the different stages of the methodology.

2.1 Modelling framework

2.1.1 The hydrological model

The hydrological model (Oasis-model) aims to simulate a variety of i-SUDS design scenarios for long climate records (> 5-yrs), to capture the variability of rainfall, soil moisture, storage availability and hydrological processes. It consists of: i) a production sub-module, to simulate a variety of runoff and pollutant emission behaviors and ii) a facility sub-module, to simulate volume reduction and its impact on pollution control (cf. Figure 1).

The principle and the main characteristics of the model are presented hereafter. A detailed description of the hydrological model is provided as supplementary material in S2.

2.1.1.1 Production sub-module

The production module was designed to cover a diversity of runoff and pollutant production behaviors from impervious surfaces. The processes considered are: rainfall, surface evaporation, infiltration, overland flow and, for pollutants, surface accumulation and wash-off.

The water balance equation associated with runoff modelling is given by:

$$\frac{dh_{prod}}{dt} = R - Q_{prod} - E_{prod} - I_{prod} \quad (1)$$

With: h_{prod} ([L]) the surface storage expressed as rainfall depth; R ([L.T^{-1}]): rainfall-rate; Q_{prod} ([L.T^{-1}]): runoff-rate; E_{prod} ([L.T^{-1}]): evaporation-rate and I_{prod} ([L.T^{-1}]): infiltration-rate. Q_{prod} is computed as $max[1/T_{prod} \times (h_{prod} - SD_{prod}), 0]$, where $1/T_{prod}$ [T^{-1}] is a retardation factor and SD_{prod} ([L]) surface depression. E_{prod} ([L.T^{-1}]) is estimated from Penman-Monteith reference evapotranspiration ET_0 ([L.T^{-1}]) using a multiplicative factor EF_{prod} ([-]). I_{prod} is calculated from a constant loss K_{prod} ([L.T^{-1}]) that may be set to zero.

Pollutant concentrations in runoff are calculated using a generic model that can describe two contrasting emission dynamics: i) particle accumulation & wash-off and ii) dissolution from building materials. It derives from an analysis of the dynamics of suspended solids from urban streets (Sage et al. 2015b) and metal leaching from metal roofs (Sage et al. 2016). Corresponding equations are given below:

$$C_{prod,t} = \frac{1}{Q_{prod,t} \times \Delta t} \times \left(M(t) \times \left[1 - e^{-C_1 \times {Q_{prod,t}}^{C_2} \times \Delta t} \right] + C_0 \times {Q_{prod,t}}^{C_3} \times \Delta t \right) \quad (2)$$

$$\frac{dM(t)}{dt} = D_{acc} \times [M_{lim} - M(t)] \quad (3)$$

With: Δt ([T]) the timestep; $C_{prod,t}$ ([M.L^{-3}]): concentration in runoff between t and $t+\Delta t$; $Q_{prod,t}$ ([L.T^{-1}]): runoff between t and $t+\Delta t$; $M(t)$ ([M.L^{-2}]): pollutant load accumulated over production area at t (calculated from (3) when $Q_{prod,t} = 0$ and updated from the term within brackets in (2) when $Q_{prod,t} > 0$); C_0, C_1, C_2 and C_3 : emission parameters; D_{acc} ([T^{-1}]): accumulation rate; M_{lim} ([M.L^{2}]): maximum $M(t)$ value.

2.1.1.2 Facility sub-module

I-SUDS are described as conceptual storage units providing volume reduction through infiltration or evapotranspiration. The processes considered are: infiltration, surface evaporation, evapotranspiration from the soil, unsaturated flow in the soil column and pollutant mixing within the storage unit. The storage unit may incorporate a flow-rate control device to simulate storage and release of captured volumes at a controlled rate (cf. Figure 2). This option is typically associated with systems that aim to prevent discharge for frequent rain events and provide peak-flow attenuation for more infrequent ones. The two configurations are later referred to as “simple volume abstraction” and “flow-rate control” designs.

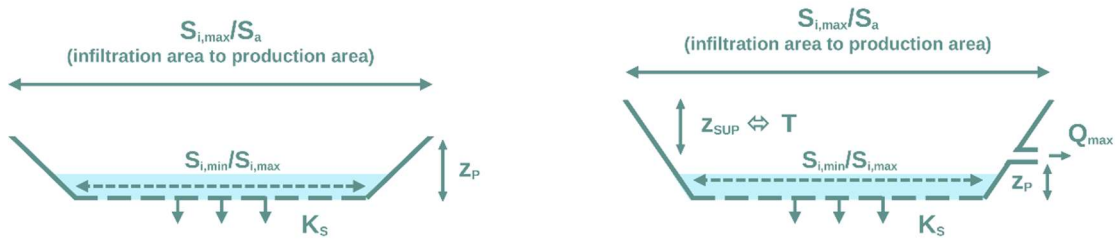

Figure 2 - Description of the facility (left- side: simple volume abstraction design; right side: flow-rate control design)

An area normalized representation of the facility is adopted: the size of the storage unit is characterized by a ratio between the maximum area available for infiltration $S_{i,max}$ ([L^2]) and the runoff production area S_a ([L^2]). The area available for infiltration is assumed to vary linearly with storage depth (trapezoidal cross section). The shape of the storage unit is thus described by a single parameter $S_{i,min}/S_{i,max}$ ([-]), representing the fraction of the facility area available for infiltration when the facility is empty. The permanent ponding depth of the system is denoted as z_P ([L]). The characteristics of the soil are captured through a single saturated hydraulic conductivity parameter K_S ([$L.T^{-1}$]) (further details are given below). Three additional parameters are introduced in the case of flow-rate control designs: a maximum allowable outflow rate Q_{max} (normalized by the runoff production area) ([$L.T^{-1}$]); a design return period T ([T]) and a maximum allowable depth z_{lim} ([L]). The supplementary depth z_{SUP} ([L]) needed to manage the rainfall volume associated with return period T is calculated from previous parameters based on intensity-duration-frequency curves at the local climate station (the procedure is detailed in S2). If the calculated value yields to a total depth greater than z_{lim}, z_{SUP} is set to z_{lim} - z_P.

The water balance within the storage unit is given by:

$$\frac{dh_f}{dt} = R + Q_{prod} \times \frac{S_a}{S_{i,max}} - I_f - E_f - Q_{out} \quad (4)$$

With: h_f ([L]) the surface storage expressed as an equivalent depth over $S_{i,max}$; I_f ([$L.T^{-1}$]): infiltration-rate; E_f ([$L.T^{-1}$]): standing water evaporation-rate; and Q_{out} ([$L.T^{-1}$]): downstream discharge-rate. E_f ([$L.T^{-1}$]) is calculated from Penman-Monteith reference evapotranspiration ET_0 ([$L.T^{-1}$]) using a multiplicative factor EF_f ([-]). For simple volume abstraction designs, Q_{out} equals the overflow-rate Q_{over} ([$L.T^{-1}$]) calculated as $max[h_f – (h_{MAX} + SD_f),\ 0] / \Delta t$, where h_{MAX} ([L]) is the maximum storage capacity (expressed as an equivalent depth) and SD_f ([L]) a surface depression parameter. For flow-rate control designs, $Q_{out} = Q_{over} + Q_{ctrl}$, where Q_{ctrl} ([$L.T^{-1}$]) is the outflow-rate from the flow-limiting device calculated as follows:

$$Q_{ctrl}(t) = \frac{S_a \times Q_{max}}{S_{i,max}} \times \left[a_1 + (1 - a_1) \times \left(\frac{\max[z - z_P, 0]}{z_{SUP}} \right)^{a_2} \right] \quad (5)$$

With: z ([L]): the water elevation in the facility (calculated from h_f) ; a_1 and a_2: parameters controlling the behavior of the flow-limiting device (a_1 >0 reflects the installation of the flow-limiting device at a lower elevation than the bottom of the facility; for a_2 = 0.5, the equation reverts to simple orifice law; Q_{max} is reached when $z = z_P + z_{SUP}$).

The infiltration term in equation (4) is calculated from the I2RS ("improved infiltration-redistribution scheme") model introduced in Sage et al. 2020, which combines the Green-Ampt infiltration equation and a 1-D unsaturated flow model to simulate soil-moisture redistribution under the effects of gravity, capillary forces, and evapotranspiration. The soil is described as a freely drained 2-m homogeneous column. So as to limit the number of input parameters in the Oasis-model, soil characteristics are captured through a single saturated hydraulic conductivity value K_S. As the I2RS model relies on the Brooks-Corey (1964) water retention and hydraulic conductivity functions, four additional hydrodynamic parameters must however be specified. The latter are calculated by performing linear interpolation (K_S-based) from reference values associated with different soil classes (Rawls et al. 1982).

At this point, it may be noted that the water balance (equation 4) is not affected by the value of $S_{i,max}$ (or S_a) itself, but by the ratio between $S_{i,max}$ and S_a. In other words, the impact of S_a and $S_{i,max}$ on the proportion of the incoming volume retained by the facility or discharged downstream, is completely captured by the $S_{i,max}/S_a$ ratio.

Pollutant concentrations in the storage unit are calculated under the assumption that runoff inflow instantaneously mixes with stored water. Specific treatment processes (such as settling or adsorption) are not accounted for and pollutant removal (at the outlet) simply results from the volume reduction associated with infiltration (i.e., pollutants are assumed to be permanently trapped in the soil). This choice can be justified by the limited contribution of treatment processes in the case of moderately contaminated runoff and their poor predictability (Bressy et al. 2014; Gavrić et al. 2019). When the maximum water elevation is reached, the pollutant mixing behavior is additionally controlled by a Boolean parameter *Byp*, which results in bypassing the storage unit (instead of causing overflow) when set to "true".

2.1.1.3 Summary of inputs and outputs

Because the purpose of the model is ultimately to support the development of a workable tool for the design of i-SUDS, a distinction is introduced between design-related parameters that the end-user is expected to manipulate and more "theoretical" modeling parameters. Design parameters here include $S_{i,max}/S_a$, K_S, z_P, Q_{max}, T, z_{lim} and $S_{i,min}/S_{i,max}$. They are later referred to as δ. The 15 remaining parameters typically aim to account for the variability that should be expected regarding some of the processes simulated by the model (runoff and pollutant production, shape of the flow-rate control relationship, magnitude of evapotranspiration…) and may also reflect a lack of confidence regarding their description. They are later referred to as θ or "uncertain" parameters.

Simulations over long rainfall periods allow generating a variety of outputs. They are classified as follows: long term volume or load reduction efficiencies; water balance indicators; daily discharged volume statistics; daily volume-reduction statistics; ponding periods statistics; soil saturation statistics and z_{SUP} (also considered as a model output). This article will mostly focus on rainfall volume reduction efficiency E (%):

$$E = 1 - V_{OUT}/V_R \quad (6)$$

Where: V_{OUT} ([L^3]) is the volume discharged at the outlet of the facility; V_R is the rainfall volume ([L^3]) received by the facility and the runoff production area.

A detailed description of the 40 outputs can be found as supplementary materials in S3.

2.1.2 Neural network emulation

Continuous modeling at sub-hourly time steps and over long periods necessarily involves non-negligible computation times. Several seconds or minutes calculations can quickly become a major hurdle in assessing the impact of uncertainty associated with model parameters. It may also limit the applicability of a given model for real world applications, especially when they involve numerous simulations (e.g., inverse problems, ensemble modeling...). A neural-network emulation of the model described above is thus adopted i) to investigate the influence of model parameters on simulation outputs and ii) for the development of the Oasis-app.

The emulation is based on feed-forward neural-networks (NN). The learning database consist of 80 000 simulations associated with a quasi-random Sobol sequence sampling of input parameters. These simulations are performed for a 15-year meteorological record (5-min precipitations and daily reference evapotranspiration disaggregated at a 5-min time-step) in Paris region. Calibration is performed for the 40 model outputs using Bayesian regularization algorithm (Beale et al. 2015), for different NN structures (variable number of hidden layers and nodes per layer). Configuration achieving the best validation results is adopted.

Each output Y_n is therefore associated with a NN-function denoted as f_n:

$$Y_n = f_n(\delta, \theta) \quad (7)$$

2.1.3 The Oasis-app

2.1.3.1 Main specifications

The motivation for the development of the Oasis-app was to provide “non-expert” users with an interface to retrieve results generated from long-period simulations with the Oasis-model and, more specifically, to relate pluriannual volume-

reduction efficiencies with a limited set of i-SUDS design parameters. Its specifications were discussed in workgroups involving representatives of local and regional authorities in charge of (storm)water management.

Flexibility rapidly appeared as one of the desired characteristics of the Oasis-app. Different "contexts of use" were identified: preliminary sizing or quick design verifications consisting in a simple evaluation of the efficiency associated with a given design scenario; more detailed analysis, involving graphical interpretation of the effect of design parameters and detailed indicators regarding i-SUDS functioning; communication and raise of professional awareness, based on graphical outputs or simple examples illustrating how i-SUDS design can be adapted to meet pluriannual volume reduction objectives. In particular, the ability to identify plausible design configurations for a user-specified pluriannual volume reduction target was expected. The Oasis-app was therefore designed to treat the pluriannual rainfall volume reduction efficiency E as another parameter and to handle a variety of situations regarding how to fill input parameters. These different contexts of use also translate into multiple stage outputs, as detailed later on. Another deemed critical feature was to generate results without noticeable calculation time; Oasis-app hence takes advantages of the NN emulation described in 2.1.2 (the approach is described in 2.1.3.3).

2.1.3.2 Operating principle

The interface of Oasis-app is shown in Figure 3. It consists of 3 panels: one dedicated to input specification (left); one to graphical outputs (upper-right); one to detailed indicators regarding i-SUDS functioning, with the 40 outputs of the Oasis-model (lower-right). The input panel involves E and the 7 design parameters δ. By default, the facility is described as a simple rectangular storage unit (dedicated to volume-reduction only). Flow-rate control design is available as an option. When activated, Q_{max}, T and z_{lim} must be specified (z_{SUP} is returned after calculation). The shape of the facility can be set from two options: a flat system design with $S_{i,min}/S_{i,max} < 1$ and a sloped bottom design (longitudinal slope) for which $S_{i,min}/S_{i,max} = 0$.

In line with the "flexibility" requirement, the user is expected to fill 1 to 3 of the first 4 input fields (regardless of the options activated). When 1 or 2 of these fields are filled, the app generates a graph from which the effect of the unspecified input can be visualized. The user may later select a specific design configuration from this graph to generate detailed indicators. When 3 of these fields are filled, the tool immediately returns the value of the unspecified input in the left panel (for instance $S_{i,max}/S_a$ from E, z_p and K_s), generates detailed indicators and provides a graph for information.

Figure 3 - Oasis-app interface (output screen for Ks = 10^{-6} m/s and after selection of the $S_{i,max}/S_a$ = 7.5% and z_p = 50mm from the graphical panel). Translation from French for the main controls and menus.

The different possibilities are listed in Table 1.

Input(s) specified		Graphical output panel	Input and detailed indicators panels
1	E	$S_{i,max}/S_a$ as a function of K_S for 3 z_P values	Returns detailed indicators after selection of a specific configuration from the graphical output panel
	$S_{i,max}/S_a$	E as a function of K_S for 3 z_P values	
	K_S	E as a function of $S_{i,max}/S_a$ for 3 z_P values	
	z_P	$S_{i,max}/S_a$ as a function of K_S for 3 E values	
2	E and $S_{i,max}/S_a$	z_P as a function of K_S	Returns detailed indicators after selection of a specific configuration from the graphical output panel
	E and K_S	z_P as a function of $S_{i,max}/S_a$	
	E and z_P	$S_{i,max}/S_a$ as a function of K_S	
	$S_{i,max}/S_a$ and K_S	E as a function of z_P	
	$S_{i,max}/S_a$ a,d z_P	E as a function of K_S	
	K_S and z_P	E as a function of $S_{i,max}/S_a$	
3	E, $S_{i,max}/S_a$ and K_S	E as a function of z_P (for information)	Directly returns z_P and detailed indicators
	E, $S_{i,max}/S_a$ and z_P	E as a function of K_S (for information)	Directly returns K_S and detailed indicators
	E, K_S and z_P	E as a function of $S_{i,max}/S_a$ (for information)	Directly returns $S_{i,max}/S_a$ and detailed indicators
	$S_{i,max}/S_a$, K_S, z_P	E as a function of $S_{i,max}/S_a$ (for information)	Directly returns E and detailed indicators

Table 1 - Behaviors of the different panels of the Oasis-app as a function the input(s) specified by the user.

2.1.3.3 Embedding simulation results within a web-app

As a design tool, the Oasis-app relies on a relatively parsimonious parameterization. System description only involves the 7 design parameters δ, whereas the Oasis-model requires specifying 15 additional uncertain parameters θ. As shown later on (3.1.1), the latter may affect simulated outputs and setting them to fixed values may not be completely sound. A specific strategy was therefore set-up to move from the 22-parameter Oasis-model to the 7-parameter Oasis-app and incorporate the variability caused by θ in the output of the Oasis-app.

Under a given design scenario δ, each Oasis-model output Y_n is described by a probability density function $f_n(\delta,\sim)$ that reflects the variability associated with θ. In the Oasis-app, this variability is captured by focusing on the 5th and 95th percentile of $f_n(\delta,\sim)$, denoted as $\tilde{f}_{n,05}(\delta)$ and $\tilde{f}_{n,95}(\delta)$. Corresponding functions $\tilde{f}_{n,05}:\delta\rightarrow \tilde{f}_{n,05}(\delta)$ and $\tilde{f}_{n,95}:\delta\rightarrow \tilde{f}_{n,95}(\delta)$ are generated from the NN-functions $f_n:(\delta,\theta)\rightarrow f_n(\delta,\theta)$ described in 2.1.2. A database consisting of 2×10^4 design configurations δ is constructed for each output Y_n. For each design configuration, 500 simulations are performed with the NN-function f_n under random θ values so as to estimate $\tilde{f}_{n,05}(\delta)$ and $\tilde{f}_{n,95}(\delta)$. NN-functions $\tilde{f}_{n,05}:\delta\rightarrow \tilde{f}_{n,05}(\delta)$ and $\tilde{f}_{n,95}:\delta\rightarrow \tilde{f}_{n,95}(\delta)$ can then be adjusted from the database, using a similar procedure as the one described in described in 2.1.2.

The use of these NN-functions in the Oasis-app depends on the output stage and inputs specified by the user. First, a conservative approach, focusing on 5th percentile values, is adopted for the volume-reduction efficiency E involved in the input and graphical output panels. For direct calculation of E from $S_{i,max}/S_a$, z_p and K_S or for the construction of graphs where E is a function of another parameter (cf. Table 1), the app directly relies on $\tilde{f}_{0,05}$ (n = 0 refers to E). When E is specified by the user, an inversion of $\tilde{f}_{0,05}:\delta\rightarrow E$ is needed. If the user specifies 3 of the first 4 input fields including E, E is evaluated from $\tilde{f}_{0,05}$ for different values of the unspecified parameter and the value associated with the user specified E target is obtained through interpolation. A similar approach is adopted for each point of the graphs that do not display E as function of another parameter. For the detailed indicators panel, lower and upper bound values are generated for all outputs (including E) based on $\tilde{f}_{n,05}$ and $\tilde{f}_{n,95}$.

Further details on the construction of these NN-functions are available as supplementary material in S4.

2.2 Diagnosis of the hydrological model

2.2.1 Sensitivity analysis

A peculiarity of SUDS model, such as the one described in the article, is that they involve two different type of input factors, i.e. explicit design-related parameters (δ) that the end-user is expected to specify and "uncertain" parameters (θ). Here, the objective of the sensitivity analysis is to understand how these uncertain parameters affect model outputs,

considering the diversity of possible design scenarios, which implies that design parameters δ cannot be treated as other parameters θ. A variance-based sensitivity analysis (Saltelli et al. 2010) is performed to assess the effect of θ over a wide range of i-SUDS design scenarios. The analysis focuses on total sensitivity indices, that measure the variance of model outputs left by leaving a given input factor X_i variable while the others ($X_{\sim i}$) are fixed:

$$S_{Ti,\delta} = \frac{E_{X_{\sim i}}[V(Y_\delta|X_{\sim i})]}{V(Y_\delta)}_{X_i \in \theta} \quad (8)$$

Where: Y_δ is model outputs for a given design scenario (i.e., specific values for δ) ; $E_{X_{\sim i}}[V(Y_\delta|X_{\sim i})]$ the expected conditional variance of Y_δ given $X_{\sim i}$; and $V(Y_\delta)$ the total variance of the outputs Y_δ. $S_{Ti,\delta}$ therefore reflects the total contribution of $X_i \in \theta$ to $V(Y_\delta)$.

The analysis is performed for 10^4 design scenarios (with and without flow-rate control) using the NN-functions described in 2.1.2. For each design scenario, $S_{Ti,\delta}$ is calculated based on the estimator of Saltelli et al. (2010) considering 10^4 samples for θ. Parameter range for δ is given in Table 2. Because random sampling of δ from this parameter range can result in unrealistically low efficiency configurations or oversized designs associated with negligible output variability, the analysis focuses on scenarios for which $50\% \leq E \leq 99\%$.

Design parameters (δ)	Lower bound	Upper bound
$S_{i,max}/S_a$ (%)	1	25
z_P (mm)	0	600 /300*
K_S (m.s^{-1})	10^{-7}	10^{-4}
Q_{max} (l.s^{-1}.ha^{-1})	1	20
T (yr)	1	50
z_{lim} (mm)	300	1500
$S_{i,min}/S_{i,max}$ (-)	0	1

*Table 2 - Lower and upper bound for design parameters (*for flow-rate control designs)*

The effect of θ is then evaluated from the distribution of $S_{Ti,\delta}$ across δ. As a relative measure of sensitivity, $S_{Ti,\delta}$ has to be interpreted with respect to total variance $V(Y_\delta)$ which is expected to vary significantly across δ. The effect of $X_i \in \theta$ is therefore evaluated from average $S_{Ti,\delta}$ values associated with inter-quartile ranges of $V(Y_\delta)$. Further details regarding the implementation of the sensitivity analysis, including parameter range for θ, are available as supplementary material in S5.

Only 4 of the 40 available outputs are considered here: i) the pluriannual rainfall volume reduction efficiency E; ii) the pluriannual pollutant load reduction efficiency ($E_{LOAD} = 1 - M_{OUT}/M_{IN}$ where M_{IN} and M_{OUT} respectively represent the pollutant load generated on the production area and discharged at the outlet of the facility in [M]); iii) the deep infiltration (DI [-]) component of the water balance, defined as the proportion of the volume collected by the facility that is evacuated

at the bottom of the soil domain (2m depth); iv) the 9th decile duration of ponding periods ($D_{PP,9}$ [T]) calculated from sorted durations of periods during which water accumulates in the facility.

2.2.2 Effect of underground conditions

The presence of a shallow groundwater (GW) or a low-permeability layer at a few meters from the soil surface can significantly reduce the performance of i-SUDS (D'Aniello et al. 2019). However, underground conditions are often poorly known at the plot scale and most design tools rely on simplistic descriptions of the soil profile, generally with the assumption that infiltrated volume can freely drain to deeper soil horizons.

Here, a coupled i-SUDS and subsurface-flow modelling approach is adopted to understand when the presence of a shallow GW or a restrictive horizon may preclude the applicability of the modeling framework described in section 3. The aim is also to highlight contexts for which special attention should be paid to underground conditions. The Oasis-model is used in combination with the 2D saturated-flow module described in Pophillat et al. (2021) to simulate shallow GW and low-permeability layer scenarios. Under this approach, the facility is described as a circular system (radial invariance) positioned at the center of a flat and circular GW flow domain. The Oasis-model provides a description of the facility and the unsaturated zone (UZ) below ground surface. The GW domain is considered as homogeneous, with same hydrodynamic properties as those specified for the UZ. Infiltration only occurs from the facility and the exchange term at the bottom of the UZ allows describing GW recharge and capillary rise. A fixed head boundary condition is adopted at the outer limit of the GW domain (100 m from the outer limit of the facility). GW bedrock may be totally impermeable (no-flux) or not (constant rate infiltration). This allows modeling: 1) infiltration over a shallow GW domain or 2) the formation of a saturated zone within the soil at the interface with a low-permeability layer. Four additional parameters are introduced: the initial GW depth Z_{GW0} [L], GW thickness H_{GW} [L], catchment area S_a (controlling the area of the facility through $S_{i,max}/S_a$) and a constant rate loss K_{bed} through the bedrock ([L.T^{-1}]).

Simulations are successively performed with the original and the coupled approach, considering multiple design scenarios and underground conditions. For shallow GW scenarios: Z_{GW0} ranges between 0.5 and 15 m, H_{GW} between 2 and 10 m and $K_{bed} = 0$. For low-permeability layer scenarios: $Z_{GW0}+H_{GW}$ (i.e., bedrock depth later denoted as Z_{bed}) ranges between 0.5 and 15 m, $H_{GW} = 10^{-2}$ m (negligible thickness) and K_{bed} is assumed to be 10 or 100 times lower than K_S. In both cases, $S_{i,max}/S_a$ ranges between 1 and 25%, z_p between 50 and 500 mm, S_a between 10^3 and 10^4 m^2. For the sake of simplicity, simulations are conducted for simple volume abstraction designs, with $S_{i,min}/S_{i,max} = 1$ and for a 5-yr period. Further details on the setup of model coupling are provided as supplementary material in S6.

4.8×10^4 shallow GW and 3.2×10^4 low-permeability layer scenarios are simulated. The analysis focuses on the primary model output E. The impact of underground conditions is assessed by identifying the depth (initial GW depth or low permeability layer depth) $Z_{\Delta E=10\%}$ beyond which the absolute difference between E as calculated with the original Oasis-model and the one obtained from the coupled approach becomes smaller than 10%.

2.3 Demonstrating the applicability of the approach

In 3.2.1, the applicability of the Oasis-app is illustrated from a selection of outputs associated with different situations regarding input specifications (considering both simple volume abstraction and flow rate control designs). Graphical outputs are first examined. The capabilities of the Oasis-app are further exposed through an examination of the detailed indicators generated for 3 contrasting design configurations, resulting in the same volume reduction efficiency.

In 3.2.2, the relevance of the approach over static design approaches, usually adopted to address pluriannual stormwater volume reduction objectives, is later assessed from a large ensemble of simulations covering a broader variety of design configurations. The analysis focuses on the "8 – 10 mm storage capacity recovered within 24 hours" rule, often substituted for the 80% rainfall volume target in Paris region (i.e., for the climate conditions considered in Oasis). 10^5 configurations are generated from quasi-random sampling for both simple volume abstraction and flow-rate control designs (using the parameter range shown in Table 2). Corresponding rainfall volume reduction efficiencies E are computed with the Oasis-app (i.e., $\tilde{f}_{0,05}$). Lower-bound estimates for the 9th decile duration of wetting periods (dWP_{90}) are also calculated to discard configurations with $dWP_{90} \geq 96$ h considered as nonfunctional. The distribution of E values as a function of time-to-empty (calculated as z_P/Ks) and the equivalent rainfall depth associated with z_P is then examined to clarify the extent to which the permanent storage targets associated with drawdown requirements can be used as a surrogate for pluriannual volume reduction objectives.

3 Results and discussion

3.1 Model testing

3.1.1 Sensitivity analysis

The results of the sensitivity analysis are shown in Table 3. Mean $S_{Ti,\delta}$ values associated with the 3 inter-quartile ranges ($Q2$, $Q3$, $Q4$) of $V(Y_\delta)$ are provided for the 15 uncertain parameters θ and 4 selected outputs. The absolute effect of θ on the variability of Y_δ is expressed by the mean value of standard deviations $|\sigma_\theta(Y_\delta)|$ associated with each inter-quartile range. The table additionally displays the average $E_\delta(Y)$ and standard deviation $\sigma_\delta(Y)$ of the 4 outputs across design scenarios.

	Rainfall volume reduction efficiency (E)			Pollutant reduction efficiency (E_{LOAD})			Deep drainage as % of captured volume (DI)			9th decile duration of watering event ($D_{PP,9}$)		
$E_\delta(Y)$	81%			77%			64%			93h		
$\sigma_\delta(Y)$	15%			19%			20%			166h		
	Q2	**Q3**	**Q4**	**Q2**	**Q3**	**Q4**	**Q2**	**Q3**	**Q4**	**Q2**	**Q3**	**Q4**
$\lvert\sigma_\theta(Y_\delta)\rvert$	1.6%	3.4%	6.1%	3.6%	6.3%	9.2%	2.1%	3.2%	5.0%	0.6h	3.2h	42h
	Mean sensitivity indices											
SD_{prod}	0.22	0.25	0.27	0.04	0.03	0.03	0.12	0.08	0.05	0.11	0.10	0.15
K_{prod}	0.20	0.24	0.26	0.01	0.01	0.01	0.16	0.15	0.10	0.26	0.23	0.23
EF_{prod}	0.02	0.03	0.04	0.00	0.00	0.00	0.04	0.02	0.05	0.02	0.04	0.02
T_{prod}	0.24	0.27	0.28	0.03	0.03	0.03	0.10	0.07	0.04	0.19	0.12	0.17
SD_f	0.02	0.01	0.01	0.01	0.00	0.01	0.01	0.02	0.02	0.06	0.07	0.03
EF_f	0.01	0.01	0.01	0.01	0.01	0.01	0.36	0.40	0.46	0.02	0.10	0.19
a_1	0.02	0.01	0.01	0.01	0.01	0.01	0.02	0.02	0.03	0.04	0.05	0.03
a_2	0.28	0.19	0.14	0.14	0.12	0.10	0.23	0.27	0.30	0.36	0.38	0.25
Byp	0.00	0.00	0.00	0.19	0.27	0.36	0.00	0.00	0.00	0.00	0.00	0.00
D_{acc}	0.00	0.00	0.00	0.10	0.10	0.12	0.00	0.00	0.00	0.00	0.00	0.00
M_{lim}	0.00	0.00	0.00	0.00	0.00	0.00	0.00	0.00	0.00	0.00	0.00	0.00
C_0	0.00	0.00	0.00	0.02	0.01	0.01	0.00	0.00	0.00	0.00	0.00	0.00
C_1	0.00	0.00	0.00	0.43	0.43	0.36	0.00	0.00	0.00	0.00	0.00	0.00
C_2	0.00	0.00	0.00	0.01	0.01	0.01	0.00	0.00	0.00	0.00	0.00	0.00
C_3	0.00	0.00	0.00	0.06	0.04	0.02	0.00	0.00	0.00	0.00	0.00	0.00

Table 3 - Mean sensitivity indices $S_{Ti,\delta}$ associated with Q2, Q3 and Q4 for the 4 selected outputs and corresponding $\lvert\sigma_\theta(Y_\delta)\rvert$ values (underlining for $S_{Ti,\delta} \geq 0.1$). The table also displays average and standard deviation value $E_\delta(Y)$ and $\sigma_\delta(Y)$ of the four selected outputs across all design scenarios

Further examination of the sensitivity indices shows that the variability of each output is dominated by a limited set of parameters. Expectedly, the variability of *E* is mostly controlled by runoff production parameters as well as the a_2 coefficient which determines "how fast" maximum allowable outflow rate is reached (and thus the ability to store water above z_P) for flow-rate control scenarios. The impact of a_2 tends to be less significant for *Q4* and *Q3* than for *Q2*, which indicates that designs resulting in largest variabilities are primarily affected by runoff production parameters. Precise assessment of *E* would therefore require explicit consideration of the hydrological behavior of production areas. However, given that the latter cannot be easily captured from observable physical catchment characteristics (Rammal and Berthier 2020), the uncertainty caused by runoff production parameters could as well be considered as acceptable in many contexts.

Regarding E_{LOAD}, a_2 remains influential whereas runoff production parameters have a much more limited effect. Large $S_{Ti,\delta}$ values are obtained for the bypass option and two of the pollutant model parameters, which indicates that the pollution-control efficiency of i-SUDS is sensitive to the temporal distribution of concentrations during rain events and to the pollutant-mixing behavior within the facility. Here, the use of a wide parameter range for the pollutant model and the description of two contrasting behaviors for pollutant-mixing result in a large variability of E_{LOAD} as compared to *E*. This suggests that focusing on hydrological performances rather than pollution-based indicators might be preferable when the

evolution of concentrations in runoff or within i-SUDS cannot be adequately anticipated. Such attitude is supported by the low reliability of pollutant concentration models in the absence of local monitoring data (Tuomela et al. 2019) and the knowledge gaps regarding processes (not limited to hydrodynamics) that can affect pollutant concentrations within i-SUDS (Gavrić et al. 2019). In the case of Oasis-model, this may be further justified by the fact that pluriannual runoff volume reduction efficiencies provide a lower bound estimate for E_{LOAD}.

As for E, the two remaining outputs are sensitive to runoff production parameters and a_2. High $S_{Ti,\delta}$ values are additionally calculated for EF_F which controls the magnitude of evapotranspiration within the facility. This suggests that a detailed description of evapotranspiration is not needed to estimate the pluriannual efficiency of i-SUDS (at least when the area of the facility is significantly lower than the runoff production area), whereas it is likely to bias the assessment of water balance or hydrological loading indicators such as DI or $D_{PP,9}$. More generally, the differences in $S_{Ti,\delta}$ between outputs or across interquartile classes as well as the non-negligible values obtained for most hydrological parameters illustrate the complexity of model's response to θ. This suggest that the effect of θ, which depends on output type and design scenario, cannot be easily anticipated and supports the adoption of methods that explicitly consider the variability introduced by these "uncertain" parameters.

3.1.2 Effect of underground conditions

The influence of S_a and K_S on the distribution of $Z_{\Delta E=10\%}$ for the shallow groundwater and low-permeability layer scenarios is shown in Figure 4.

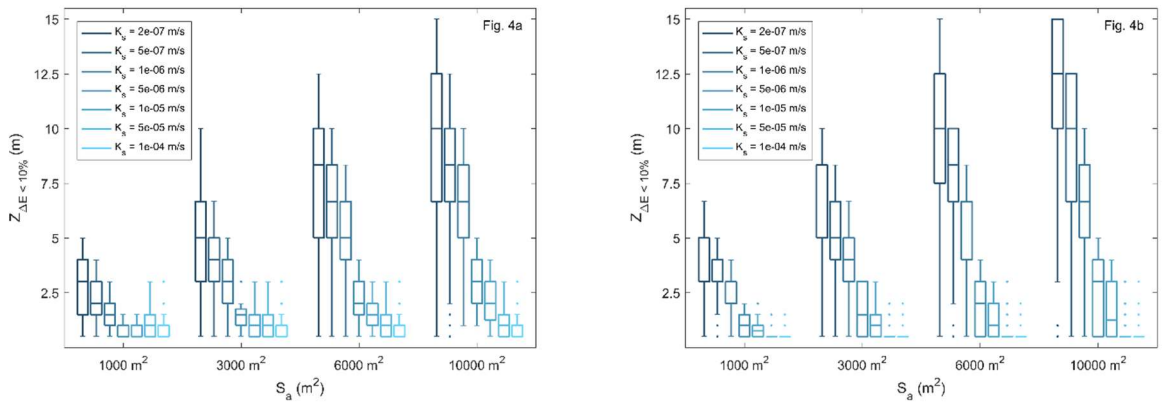

Figure 4 - Box plot for $Z_{\Delta E=10\%}$ as a function of S_a and soil saturated hydraulic conductivity K_S for the shallow GW (Fig. 4a) and low-permeability layer (Fig. 4b) scenarios

In both scenarios, $Z_{\Delta E=10\%}$ exhibits a strong dependance on S_a resulting from the direct influence of S_a on $S_{i,max}$ through $S_{i,max}/S_a$. Since the potential contribution of lateral GW flow to the dissipation of infiltrated flow decreases as the size of the facility increases, $Z_{\Delta E=10\%}$ increases as S_a (i.e. $S_{i,max}$) increases. The influence of S_a is particularly marked for $K_S \leq 5\times10^{-}$

^{6} m/s and becomes more limited as the permeability of the soil domain increases. The effect of K_S here primarily results from its control on GW transmissivity. For a given S_a value, $Z_{\Delta E=10\%}$ thus decreases as K_S increases. The effect tends to be more pronounced for the low-permeability layer scenario, as K_S additionally controls the losses through the bedrock through K_{bed} (set to K_s/10 or K_s/100). In both cases, $Z_{\Delta E=10\%}$ only reaches the upper bound of Z_{GW0} (15 m) for the least favorable configurations (S_a = 10 000 m^2 with the least permeable materials). For medium to high permeability values (K_S $\geq 5\times10^{-6}$ m/s) or small catchment areas (S_a = 1000 m^2), $Z_{\Delta E=10\%}$ rarely exceeds few meters.

As shown in Figure 5, $Z_{\Delta E=10\%}$ exhibits a non-linear relation with $S_{i,max}/S_a$: low $S_{i,max}/S_a$ values result in a more spatially concentrated inflow, increasing the potential for interactions with GW (high Z_{GW0}), but also potentially lower infiltration volumes, counterbalancing the effect of inflow concentration (especially for low K_S); oppositely, high $S_{i,max}/S_a$ values result in a less concentrated inflow, but also potentially higher infiltration volume (resulting in high $Z_{\Delta E=10\%}$ for low K_S). The differences between median and maximum $Z_{\Delta E=10\%}$ values reflect the variability associated with remaining parameters (S_a, z_P and H_{GW}, in the case of shallow GW scenarios). In the case of shallow GW scenarios, H_{GW} governs GW transmissivity and is thus negatively correlated with $Z_{\Delta E=10\%}$ (Spearman's rank correlation coefficient ρ = -0.15). The relation between $Z_{\Delta E=10\%}$ and z_P is more complex as the latter not only controls infiltration volumes but also the ability to temporary retain water above the soil surface and thus compensate for reduced infiltration capacities (no significant correlation with $Z_{\Delta E=10\%}$).

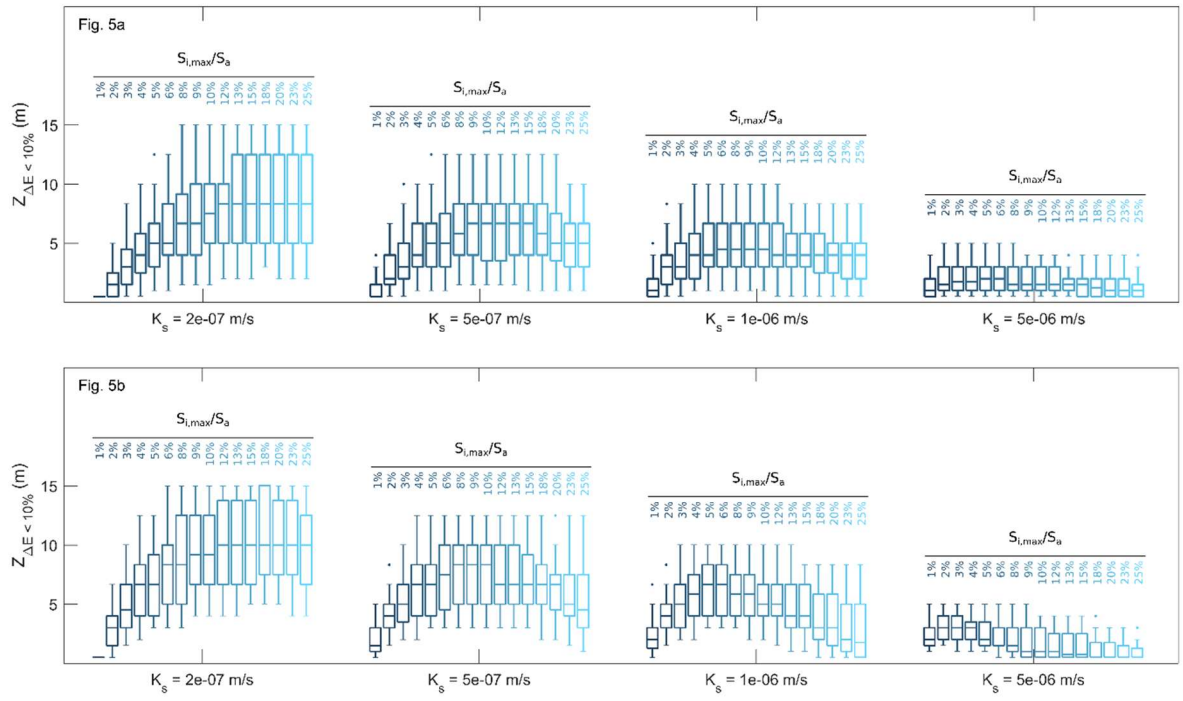

Figure 5 - Median and maximum values of $Z_{\Delta E=10\%}$ as a function of K_S for the shallow GW (Fig. 5a) and low-permeability layer (Fig. 5b) scenarios for K_S values between 2×10^{-7} and 5×10^{-6} m/s

The range of $Z_{\Delta E=10\%}$ values calculated for the different scenarios suggests that the use of a tool such as Oasis-model may often require an elementary characterization of *GW* conditions and subsurface materials. Results evidence the potentially non-linear and non-monotonic effects of design parameters and underground conditions on the distance below which a shallow GW or a low-permeability layer is likely to affect the performance of i-SUDS. While identifying a minimum acceptable distance to GW or low permeability layer for a specific configuration may not be straightforward, previous analysis nevertheless provides a basis to tell out when Oasis may be applied or not. Because it involves assumptions (flat bedrock, fixed-head boundary condition at the outer limit of the GW domain, no consideration of potential lateral anisotropy…) that potentially exacerbate GW elevations below the facility, $Z_{\Delta E=10\%}$ values should presumably be interpreted as upper-bounds for the minimum distance to shallow GW or low permeability layer. Similarly, in the case of shallow GW scenarios where annual fluctuations are generally expected (instead of constant level as in the simulation), comparison of $Z_{\Delta E=10\%}$ to a high water-level or winter GW elevation would represent a conservative approach.

Given the importance of S_a and K_S, recommendations regarding the applicability of the Oasis-app with respect to underground conditions are provided as a range of admissible distances to shallow GW or low-permeability layer for different S_a and K_S values as shown in Table 4:

	K_S			**K_S**		
	10^{-7} to 10^{-6} m.s^{-1}	**10^{-6} to 10^{-5} m.s^{-1}**	**10^{-5} to 10^{-4} m.s^{-1}**	**10^{-7} to 10^{-6} m.s^{-1}**	**10^{-6} to 10^{-5} m.s^{-1}**	**10^{-5} to 10^{-4} m.s^{-1}**
S_a	**Distance to GW (m)**			**Distance to low permeability layer (m)**		
0.1 ha or less	2 to 5	1 to 3	1 to 3	3 to 6.5	1.5 to 4	0.5 to 1.5
0.1 to 0.3 ha	3 to 8.5	1 to 5	1 to 3	4 to 10	1.5 to 6.5	0.5 to 2.5
0.3 to 0.6 ha	5 to 12.5	2 to 6.5	1 to 3	6.5 to 15	2 to 8.5	0.5 to 3
0.6 to 1 ha	6.5 to 15	3 to 10	1 to 3	8.5 to >15*	3 to 10	0.5 to 4

*Table 4 - Range of admissible distance to GW or low-permeability layer as function of S_a and K_S for the application of the Oasis-app (based on 50 and 99th percentile values of $Z_{\Delta E=10\%}$ for each Sa and K_S class) (*Influence expected above 15 m)*

3.2 Applicability of the Oasis-app to meet volume reduction targets

3.2.1 Illustration from a selection of outputs

Figure 6a shows the graphs returned to the user when specifying an 80% volume reduction target and leaving other input fields (including flow-rate control option) empty. $S_{i,max}/S_a$ is given as a function of K_S for different z_P values, allowing the user to visualize how the design of i-SUDS may be adjusted to meet E = 80%. Here, the use of K_S on the x-axis can also help to understand the design implications of the potentially large uncertainties associated with this parameter. Similarly, Figure 6b shows the graph produced by the Oasis-app when additionally setting K_S to 5×10^{-7} m.s^{-1} (i.e. assuming the latter

was accurately estimated) and enabling the flow-rate control option (Q_{max} = 3 l/s/ha, T = 10 years and z_{SUP} = 600 mm). In this case, z_P is given as a function of $S_{i,max}/S_a$ allowing the user to select pairs of values consistent with specified inputs.

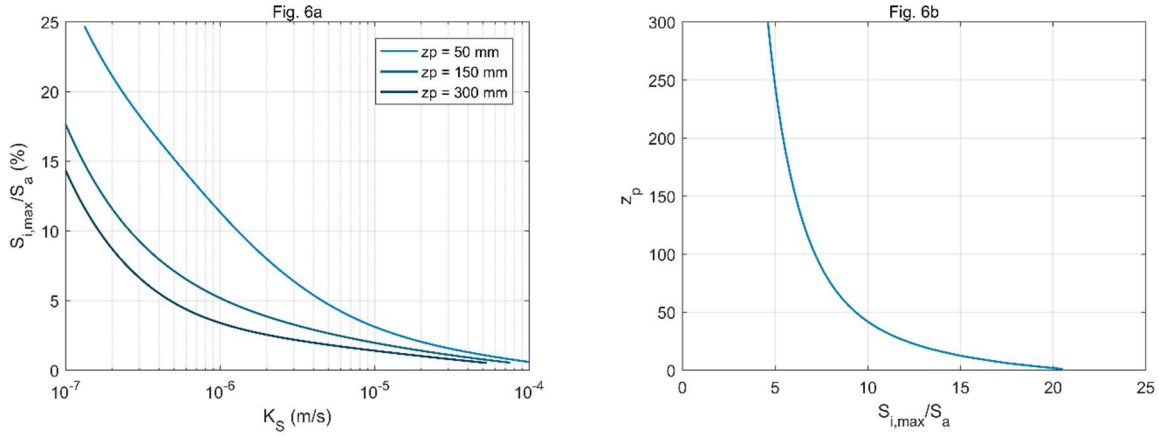

Figure 6 - Graphical outputs generated by the Oasis-app for two different cases. 6a: E set to 80% while leaving other input fields empty (flow-rate control option disabled). 6b: E set to 80% and K_S set to 5×10^{-7} m.s^{-1} (z_P and $S_{i,max}/S_a$ not specified), flow-rate control option enabled with Q_{max} = 3 l/s/ha, T = 10 years, z_{lim} = 600 mm.

The Oasis-app offers the possibility to select specific design configurations from output graphs to generate more detailed results regarding i-SUDS performance and functioning. The results associated with 3 different configurations are presented in Table 5. Configurations 1 and 2 consist in "simple volume abstraction" designs (Figure 6a) with contrasting soil permeability. Configuration 3 consist in a "flow-rate control" design (Figure 6b) with the same permeability as configuration 1. The results are shown in Table 5.

While sharing the same lower bound estimate, the ranges of the pluriannual rainfall volume reduction efficiencies (E) differ across the 3 configurations, revealing larger uncertainties for $K_S = 5\times10^{-7}$ than for $K_S = 2\times10^{-5}$. Runoff volume reduction efficiency (proportion of runoff removed by the system) is less variable than E, which suggests that focusing on this indicator might as well be relevant. In accordance with the results presented in 3.1.1, pollutant load reduction efficiencies are more uncertain than the two above-mentioned indicators and systematically greater than or equal to runoff volume reduction efficiencies. Daily discharge volumes associated with the 1-, 6- and 12-months return periods significantly vary from a configuration to another. Similarly, the minimum expected daily volume reductions for the 4-, 8- and 16-mm thresholds (defined 5th percentile of the difference between rainfall and outflow for days with more than 4-, 8- and 16-mm) potentially differ across the 3 configurations. These differences suggest that event-based or frequency-based indicators can only be used as rough surrogates for pluriannual volume reduction efficiencies. Besides, the relatively large uncertainty associated with these indicators advocates for focusing on other performance metrics. Expectedly, the percentage of time with water in the facility (over the modelling period) as well as the median and 9th decile duration of

wetting periods (defined as continuous periods with water in the facility) are larger for low K_S (config. 1 and 3) and maximum in the case of the flow-rate control design (config. 3) as a result of the additional storage z_{SUP} above z_P as well as the lower $S_{i,max}/S_a$. These durations differ from simple time-to-drain estimates (computed as z_P/K_S) and provide a valuable information regarding i-SUDS functioning.

Design parameters	**Config. 1**	**Config. 2**	**Config. 3**
$S_{i,max}/S_a$	15.2 %	1 %	9.5 %
z_P	50 mm	300 mm	50 mm
K_S	5×10^{-7} m/s	2×10^{-5} m/s	5×10^{-7} m/s
Q_{max}	/	/	3 l/s/ha
T	/	/	10 years
z_{SUP}	/	/	600 mm
Detailed indicators		**Results**	
Pluriannual rainfall volume reduction efficiency	80 - 91 %	80 - 86 %	80 - 89 %
Pluriannual runoff volume reduction efficiency	82 - 84 %	71 - 76 %	73 - 79 %
Pluriannual pollutant load reduction efficiency	83 - 98 %	73 - 95 %	79 - 98 %
Daily discharge for the 1-mth return period*	0 - 1 mm	2 - 3 mm	2 - 4 mm
Daily discharge for the 6-mth return period*	11 to 14 mm	8 to 10 mm	10 - 13 mm
Daily discharge for the 12-mth return period*	18 to 19 mm	18 to 19 mm	12 - 18 mm
Minimum expected daily volume reduction for P ≥ 4 mm*	4 mm	4 mm	3 - 4 mm
Minimum expected daily volume reduction for P ≥ 8 mm*	8 mm	5 - 6 mm	5 - 8 mm
Minimum expected daily volume reduction for P ≥ 16 mm*	6 - 8 mm	6 - 8 mm	8 - 11 mm
Minimum expected daily volume reduction for P ≥ 20 mm*	4 - 7 mm	6 - 7 mm	7 - 12 mm
Percentage of time with water in the facility	6 - 9 %	3 -5 %	7 - 12 %
Median duration of wetting periods	3 - 4 h	2 h	5 - 7 h
9th decile duration of wetting periods	20 - 27 h	8 h	37 - 49 h
Equivalent storage and time to drain indicators			
Storage expressed as an equivalent rainfall depth (mm)	6.6 mm	3.0 mm	4.33 mm
Time-to-empty calculated as z_P /Ks (h)	28 h	4 h	14 h

*Table 5 - Example of detailed indicators calculated by Oasis for 3 different configurations associated with an 80% rainfall volume reduction efficiency (*Calculated from daily outflow volume series)*

3.2.2 Relevance over static design approaches

The 10^5 design configuration considered for the analysis are represented in a plane where x-axis is time-to-empty (drawdown, calculated as z_P/K_S) and y-axis the storage capacity associated with z_P expressed as an equivalent rainfall depth, using a different color for E<80% and $E \geq 80\%$ (Figure 7).

The analysis shows that providing an 8-mm or greater equivalent storage capacity with $z_P/K_S \leq 24$h does ensure the 80% rainfall volume reduction objective is met. However, $E \geq 80\%$ is also achieved in numerous configurations that do not meet the "8 – 10 mm storage capacity recovered within 24 hours" rule. The latter is based on the premise that intercepting this amount of rainfall each day would result in an approximately 80% volume reduction at the annual scale. By essence, the approach therefore neglects the dynamic nature of rainfall and hydrologic losses as well the variability of storage and

soil moisture conditions. In practice, the daily volume reduction that can be achieved through a permanent storage volume is very likely to be unevenly distributed at the annual scale. Trying to systematically ensure an 8 – 10 mm volume reduction, may hence often result in larger daily volume reduction and eventually yield to $E > 80\%$. Obviously, $E \geq 80\%$ objective may also be reached with storage capacities lower than 8 – 10 mm, provided that hydrologic losses are sufficient.

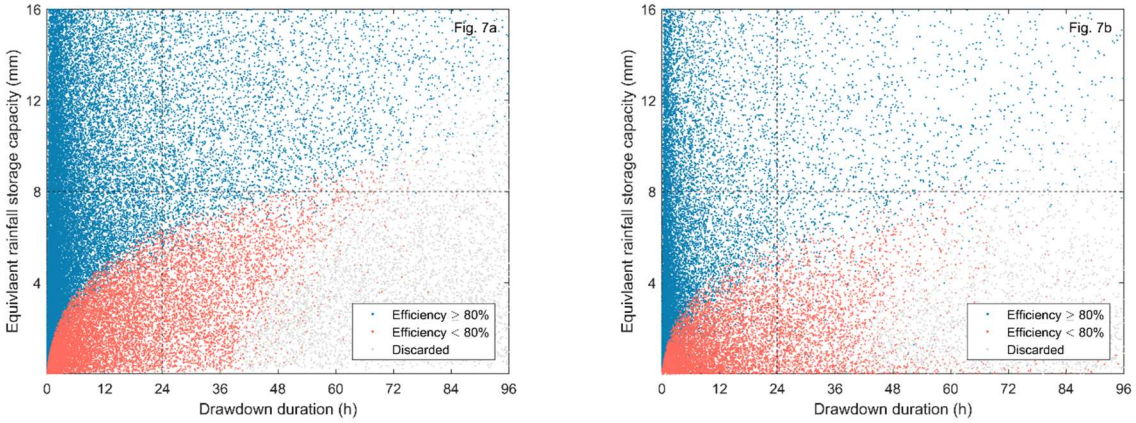

Figure 7 - Relation between the "8 – 10 mm storage capacity recovered within 24 hours" rule and the E = 80% target. 6a: simple volume abstraction design; 6b: flow-rate control design. Dashed black lines shows time-to-empty = 24h and equivalent storage depth = 8mm. Discarded configurations are those associated with $dWP_{90} \geq 96$ h

Similarly, the $z_P/K_S = 24$h requirement does not account for rainfall distribution and only partially captures the ability to recover storage capacity (as it omits the fact that infiltration rates are often higher than K_S). As shown in Figure 7, this value is presumably too stringent and $z_P/K_S = 48$h would probably be more appropriate.

The conservative nature of the "8 – 10 mm storage capacity recovered within 24 hours" rule is here exacerbated by the fact that E values computed by the Oasis-app not only reflect the hydrologic losses within the facility but also those associated with the production area. While the "8 – 10 mm" target could possibly be adapted through (a necessarily questionable) runoff coefficient to account for the losses on urban surfaces, the situation does not invalidate the above analysis. Finally, comparison between Figure 7a and Figure 7b shows that the area covered by $E \geq 80\%$ is larger for flow-rate control than simple volume abstraction scenarios. The inability of a sole combination of storage and z_P/K_S targets to capture the pluriannual volume reduction efficiency is in this case reinforced by the volume reduction provided by the additional storage z_{SUP} above z_P.

4 Conclusions

A framework (Oasis) consisting of a hydrological model (Oasis-model), a set of neural-network (NN) emulators and a web-app (Oasis-app) dedicated to the evaluation of the long-term volume reduction efficiencies of on-site infiltration

systems (i-SUDS), was introduced. A relatively original method, relying on NN-emulation, to incorporate the results of the hydrological model within the web-app while simultaneously reducing the parameter requirements, was presented. A diagnosis of the hydrological model was conducted to evaluate the impact of its parameterization and specify its domain of validity in terms of underground conditions. The applicability of the web-app was finally illustrated from a selection of outputs and its relevance over more elementary design approaches was discussed based on the analysis of large simulation ensembles, covering a variety of design configuration.

While the article primarily aims at describing a specific modelling framework for i-SUDS design, it also provides more general insights for the modelling of on-site stormwater management systems. The findings can be summarized as follows:

- Despite a relatively simple model structure, the outputs of the Oasis-model showed a complex response to the various input parameters. The sensitivity of the model to a given non-design parameter was found to depend on both the output considered and the i-SUDS design configuration, thereby highlighting a specific difficulty of sensitivity analysis for models aiming to depict a broad range of system functioning. The benefits of separating design and non-design parameters in the sensitivity analysis process to analyze the variability caused by uncertain parameters across the diversity of possible design scenarios were pointed out. The impact of non-design parameters was found to be significant and hardly predictable, which advocates for explicitly considering the uncertainty they introduce in model outputs.

- Distances below which a shallow groundwater (GW) or a low permeability layer would significantly affect the volume reduction efficiency of i-SUDS as calculated by the Oasis-model were identified for a variety of hydrogeological contexts and design configurations. These distances were found to primarily depend on the size of the infiltration system, the permeability of the soil media and GW thickness for shallow GW scenarios. Highest values (several meters) were obtained in the case of low permeability soils ($K_S \leq 5\times10^{-6}$ m/s) and large facilities (runoff production area ≥ 1000 m^2). For these configurations, the analysis highlights the limitations of a simplistic description of the soil profile (such as the one adopted in the Oasis-model as well as in other design tools) where infiltrated volumes freely drain to deeper soil horizons. It more generally evidences the potential importance of underground conditions, often poorly known at the plot scale, in i-SUDS design.

- NN-emulation was adopted to replicate the outputs of the Oasis-model at a low computational cost and to overcome some limitations of "real time" hydrologic calculations. Its implementation in the Oasis-app enabled features such as the optimization of design parameters from user-specified pluriannual volume reduction

objectives or the generation of graphs to visualize the relation between design parameters and pluriannual volume reduction efficiencies. NN-emulation also allowed handling the "uncertain" parameters of the Oasis-model and capturing their impact on the results for a given design configuration. A methodology was developed to derive NN-functions providing lower and upper bound estimates of each output as a sole function of design parameters. The approach, yet rudimental, illustrates the potential of NN-emulation for the development of design tools that explicitly consider parametric uncertainty.

- The shortcomings of static design rules based on the combination of permanent storage and drawdown targets were illustrated from an analysis performed over a variety of design scenarios under the climate conditions considered in Oasis. While such approaches were shown to potentially ensure a minimum pluriannual volume reduction efficiency, their inability to fully capture pluriannual volume reduction efficiency was evidenced. In many cases, these rules would hence represent a conservative approach and result in larger efficiencies than expected. As a reason, the use of design tools relying on continuous modelling, such as Oasis-app, should be preferred to capture the volume-reduction performance of i-SUDS and avoid oversizing or discarding satisfactory design configurations.

- The Oasis framework provides an example of transfer from a hydrological model to a decision support-tool for i-SUDS design. While the Oasis-model in itself remains relatively close to other well established SUDS models regarding the description of the hydrological processes, the Oasis-app includes several "non-standard" features as compared to existing SUDS design calculators. It first offers a flexible environment to investigate the relation between i-SUDS design and long-period volume reduction efficiencies, with few assumptions regarding inputs specification. It takes advantage of NN-emulation to mobilize results from continuous modeling in the resolution of optimization problems or the generation of graphs involving large number of simulations. It also allows computing detailed indicators related to i-SUDS functioning, with an elementary assessment of parametric uncertainty.

It is important to recall that the development of Oasis-app was first and foremost a response to local needs. As such, it aimed to provide a fit-for-purpose framework for the design of i-SUDS in Paris region. The choices made regarding the operating principle of the Oasis-app thus largely reflect the local approach to stormwater management design and the preferences of the stakeholders involved. This specialization is a trait of many calculators (such as, for example, CAD-LID-ST or SWC) designed to support local, regional, or national stormwater management goals.

The main limitations of the Oasis-app currently lie in its range of applicability regarding SUDS type, climate, and catchment conditions. Regarding climate, its validity domain is currently limited to conditions that do not differ too much from those of the Paris region. This type of limitation is an inherent characteristic of calculators that do not rely on user specified rainfall and potential evapotranspiration time series and also applies to other calculators such as CAD-LID-ST (California only) or SWC (US only). On this point, extending the applicability of the Oasis-app to other regions of France (e.g., allowing the user to select the appropriate climate station, as in SWC) is a short-term development perspective. Regarding SUDS type and catchment conditions, the Oasis-app clearly offers more limited possibilities than other calculators (such as CAD-LID-ST or SWC). While a direct integration of other SUDS type in the Oasis-app may not be easily conducted, the framework could nevertheless be adapted to more complex systems such as, for instance, bioretention cells. Because a larger number of design parameters would be needed to characterize such systems, restraining the inputs to the most important ones could probably be appropriate (drawing for instance on the method adopted in CAD-LID-ST, where optimization can be conducted for different families of bioretention designs). Similarly, catchment conceptualization could potentially be modified to account for a larger variety of production areas (following the example of CAD-LID-ST, where "self-treating areas" such as green-roofs or vegetated surfaces, likely to be implemented upstream i-SUDS, can be specified through a dedicated panel). Given the potential importance of shallow GW or low-permeability layer on i-SUDS functioning, the opportunity of more explicitly addressing the issue of underground conditions in the Oasis-app might as well be evaluated. More generally, attention should be paid to the feedback from current users in order to identify and prioritize the evolutions of the Oasis-app.

Despite the above-mentioned limitations, the Oasis-app does exhibit features that are not available in current calculators (such as SWC or CA-LID-ST) and could be relevant in other regions of the world. For instance, the use of NN-emulation allows optimizing different design parameters from a pluriannual volume reduction target (which is only possible for area parameter in CA-LID-ST and not possible at all in SWC). NN-emulation also allows generating almost instantaneously detailed indicators on SUDS functioning, while accounting for parametric uncertainty (which is neither possible with SWC or CA-LID-ST). While all the sources needed to achieve this are freely available online, direct transposition of the tool to other regions in the world may however not be desirable. First, because stormwater management approaches and regulations may vary from a place to another, the characteristics of SUDS design tools should presumably be discussed locally to better meet local practices and expectations. In addition, extension to "more demanding" climates, cold or arid for example, could possibly require reconsidering the structure of the hydrological model that was primarily designed for temperate conditions (i.e., no-snow, relatively limited contribution of evapotranspiration…). Hence, the transferability of

the Oasis-app to other regions should rather be seen in the fact that it can serve as a basis for the development of similar design tools or the improvement of existing ones.

Statements and declaration

Acknowledgement

This research was carried out under the OPUR research program. Model development was supported by the French Ministry of the Environment. The development of the web-app was supported by the Seine Normandie Water Agency. Authors gratefully acknowledge OPUR partners (Seine-Normandy Water Agency, Val-de-Marne Departmental Council, Seine-Saint-Denis Departmental Council, Hauts-de-Seine Departmental Council, Seine-et-Marne Departmental Council, City of Paris and the Interdepartmental Association for Sewerage Services in the Paris Metropolitan Area) for their support.

Competing interest

The authors have no relevant financial or non-financial interests to disclose.

Author contributions

The article was written by J. Sage and reviewed by E. Berthier, G. Chebbo, M-C. Gromaire. The hydrological model developed by J. Sage under the supervision of E. Berthier and M-C. Gromaire. J. Sage, E. Berthier, G. Chebbo, M-C. Gromaire were involved in the definition and the development of the Oasis-app.

Data availability

The Oasis-app accessible at: https://oasis.cerema.fr

The Oasis code is freely available at: *https://doi.org/10.5281/zenodo.7413958*

Databases and other tools can be made available upon reasonable request.

Notation

Variables used in both production and facility sub-modules	
R	Rainfall-rate ([L.T^{-1}])
ET_0	Penman-Monteith reference evapotranspiration ([L.T^{-1}])

t	Time ([T])
Δt	Time-step ([T])
Production sub-module related	
S_a	Area of the production area ([L^2]) (not used for calculations)
h_{prod}	Surface storage over the production area expressed as rainfall depth ([L])
Q_{prod}	Area normalized runoff-rate over the production area ([$L.T^{-1}$])
E_{prod}	Evaporation-rate over the production area ([$L.T^{-1}$])
I_{prod}	Infiltration-rate over the production area ([$L.T^{-1}$])
T_{prod}	Retardation factor used for the calculation of Q_{Prod} ([T^{-1}])
EF_{prod}	Multiplicative factor for the calculation of E_{prod} from ET_0 ([-])
K_{prod}	Constant loss rate for the calculation of I_{prod} ([$L.T^{-1}$])
$C_{prod,t}$	Pollutant concentration in runoff between t and $t+\Delta t$ ([$M.L^{-3}$])
$Q_{prod,t}$	Runoff-rate associated with the production area between t and $t+\Delta t$ ([$L.T^{-1}$])
$M(t)$	Area normalized pollutant load accumulated over production area at t ([$M.L^{-2}$])
C_0	Parameter of the pollutant concentration model (unit depends on C_3)
C_1	Parameter of the pollutant concentration model (unit depends on C_2)
C_2	Parameter of the pollutant concentration model ([-])
C_3	Parameter of the pollutant concentration model ([-])
D_{acc}	Accumulation rate ([T^{-1}])
M_{lim}	Maximum pollutant load accumulated over production area ([$M.L^2$])
Facility sub-module related	
$S_{i,max}$	Maximum area available for infiltration ([L^2])
$S_{i,min}$	Area available for infiltration when the storage unit is empty ([L^2])
z_P	Permanent ponding depth ([L])
K_S	Saturated hydraulic conductivity of the soil ([$L.T^{-1}$])
Q_{max}	Maximum allowable outflow rate (normalized by the production area) ([$L.T^{-1}$])
T	Design return period T for flow-rate control ([T])
z_{SUP}	Supplementary depth for the storage of the rainfall volume associated with T ([L])
z_{lim}	Maximum allowable depth, i.e., maximum value for $z_P + z_{SUP}$ ([L])
h_f	Surface storage in the facility expressed as an equivalent depth over $S_{i,max}$ ([L])
I_f	Infiltration-rate in the facility ([$L.T^{-1}$])
E_f	Standing water evaporation-rate in the facility ([$L.T^{-1}$])
Q_{out}	Downstream discharge-rate normalized by $S_{i,max}$ ([$L.T^{-1}$])
Q_{over}	Overflow-rate normalized by $S_{i,max}$ ([$L.T^{-1}$])
Q_{ctrl}	Outflow-rate from the flow limiting device normalized by $S_{i,max}$ ([$L.T^{-1}$])
EF_f	Multiplicative factor for the calculation of E_f from ET_0 ([-])
h_{MAX}	Maximum storage capacity expressed as an equivalent depth over $S_{i,max}$ ([L])
SD_f	Surface depression storage in the facility ([L])
z	Elevation associated with h_f ([L])
a_1	Offset parameter for the activation of the flow limiting device ([L])
a_2	Shape parameter for the calculation of Q_{ctrl} ([-])
Byp	Parameter controlling the pollutant mixing behavior when the storage unit is full ([-])
Model outputs	
E	Rainfall volume reduction efficiency ([-])

V_R	Rainfall volume received by the facility and the runoff production area ([L^3])
V_{OUT}	Volume discharged at the outlet of the facility ([L^3])
E_{LOAD}	Pollutant load reduction efficiency ([-])
M_{IN}	Pollutant load generated on the production area ([M])
M_{OUT}	Pollutant load discharged at the outlet of the facility ([M])
DI	Proportion of the volume received by facility that exfiltrates below 2m ([-])
$D_{PP,9}$	9th decile duration of ponding periods ([T])
Neural-network emulation related	
Y_n	Generic notation for model outputs (nth output)
δ	Generic notation for design parameters
θ	Generic notation for uncertain (i.e., non-design) parameters
f_n	Neural network (NN) function associated with the calculation of Y_n
$f_n(\delta,\sim)$	Distribution of Y_n at δ given the uncertainty on δ
$\tilde{f}_{n,05}$	NN-function associated with the calculation of the 5th percentile of $f_n(\delta,\sim)$
$\tilde{f}_{n,95}$	NN-function associated with the calculation of the 95th percentile of $f_n(\delta,\sim)$
Sensitivity-analysis related	
X_i	Generic notation for the ith input variable of a model
$X_{\sim i}$	Generic notation for all input variables of a model but the ith one
Y_δ	Generic notation for output variables at δ
$S_{Ti,\delta}$	Total sensitivity index associated with the X_i at δ
Underground conditions related	
Z_{GW0}	Initial GW depth ([L])
H_{GW}	Initial GW thickness ([L])
Z_{bed}	Bedrock depth ([L])
K_{bed}	Loss-rate for bedrock material ([L.T^{-1}])
$Z_{\Delta E=10\%}$	Depth beyond which GW or low-permeability layer cause less than 10% difference in E

Supplementary materials

Additional references explanations regarding SUDS design objectives adopted in Paris region (S1); detailed description of the Oasis-model (S2); description of the 40 outputs of the Oasis-model and Oasis-app (S3) ; additional details regarding the calculation of Oasis outputs (S4) protocol for sensitivity analysis implementation (S5) and setup for the coupling between the Oasis-model and the simple groundwater flow module (S6) are available online in the ASCE Library (www.ascelibrary.org).

References

Beale, M. H., M. T. Hagan, and H. B. Demuth. 2015. "Neural Network Toolbox™ User's Guide."

Beck, N. G., G. Conley, L. Kanner, and M. Mathias. 2017. “An urban runoff model designed to inform stormwater management decisions.” *Journal of Environmental Management*, 193: 257–269. https://doi.org/10.1016/j.jenvman.2017.02.007.

Bressy, A., M.-C. Gromaire, C. Lorgeoux, M. Saad, F. Leroy, and G. Chebbo. 2014. “Efficiency of source control systems for reducing runoff pollutant loads: Feedback on experimental catchments within Paris conurbation.” *Water Research*, 57: 234–246. https://doi.org/10.1016/j.watres.2014.03.040.

Brooks, R., and A. Corey. 1964. “Hydraulic properties of porous media.” *Hydrology Papers, Colorado State University*, 3: 37 pp.

Butler, D., C. James Digman, JW. Davies, and C. Makropoulos. 2018. *Urban Drainage (4th edition)*.

Chocat, B., and F. Salmoun. 2019. “Parapluie : un système gratuit d’aide au choix et à la conception des solutions de gestion des eaux pluviales à la parcelle.” *Revue L’Eau, L’Industrie, Les Nuisances*, (418): 61–64. Johanet.

CSU. 2019. *California Phase II LID Sizing Tool Documentation Manual*. 77. California State University, Office of Water Programs.

D’Aniello, A., L. Cimorelli, L. Cozzolino, and D. Pianese. 2019. “The Effect of Geological Heterogeneity and Groundwater Table Depth on the Hydraulic Performance of Stormwater Infiltration Facilities.” *Water Resources Management*, 33 (3): 1147–1166. https://doi.org/10.1007/s11269-018-2172-5.

DRIEE. 2020. *Guide technique pour l’instruction des dossiers d’eaux pluviale [Technical guide for the instruction of stormwater permits]*. Direction Régionale et Interdépartementale de l’Environnement et de l’Energie.

Ferrans, P., M. N. Torres, J. Temprano, and J. P. Rodríguez Sánchez. 2022. “Sustainable Urban Drainage System (SUDS) modeling supporting decision-making: A systematic quantitative review.” *Science of The Total Environment*, 806: 150447. https://doi.org/10.1016/j.scitotenv.2021.150447.

Fletcher, T. D., W. Shuster, W. F. Hunt, R. Ashley, D. Butler, S. Arthur, S. Trowsdale, S. Barraud, A. Semadeni-Davies, J.-L. Bertrand-Krajewski, P. S. Mikkelsen, G. Rivard, M. Uhl, D. Dagenais, and M. Viklander. 2014. “SUDS, LID, BMPs, WSUD and more – The evolution and application of terminology surrounding urban drainage.” *Urban Water Journal*, 1–18. https://doi.org/10.1080/1573062X.2014.916314.

Gavrić, S., G. Leonhardt, J. Marsalek, and M. Viklander. 2019. “Processes improving urban stormwater quality in grass swales and filter strips: A review of research findings.” *Science of The Total Environment*, 669: 431–447. https://doi.org/10.1016/j.scitotenv.2019.03.072.

Kaykhosravi, S., U. T. Khan, and A. Jadidi. 2018. “A Comprehensive Review of Low Impact Development Models for Research, Conceptual, Preliminary and Detailed Design Applications.” *Water*, 10 (11). https://doi.org/10.3390/w10111541.

MPCA. 2022. “Minnesota Stormwater Management Manual.” *Minnesota Stormwater Management Manual website (Minnesota Pollution Control Agency)*. Accessed April 29, 2022. https://stormwater.pca.state.mn.us.

Nie, L., H. Jia, K. Zhang, and F. Guangtao. 2020. *Assessment Standard for Sponge City Effects*. IWA Publishing.

Pophillat, W., J. Sage, F. Rodriguez, and I. Braud. 2021. “Dealing with shallow groundwater contexts for the modelling of urban hydrology – A simplified approach to represent interactions between surface hydrology, groundwater and underground structures in hydrological models.” *Environmental Modelling & Software*, 144: 105144. https://doi.org/10.1016/j.envsoft.2021.105144.

Qi, Y., F. K. S. Chan, C. Thorne, E. O’Donnell, C. Quagliolo, E. Comino, A. Pezzoli, L. Li, J. Griffiths, Y. Sang, and M. Feng. 2020. “Addressing Challenges of Urban Water Management in Chinese Sponge Cities via Nature-Based Solutions.” *Water*, 12 (10): 2788. https://doi.org/10.3390/w12102788.

Rammal, M., and E. Berthier. 2020. “Runoff Losses on Urban Surfaces during Frequent Rainfall Events: A Review of Observations and Modeling Attempts.” *Water*, 12 (10). https://doi.org/10.3390/w12102777.

Rawls, W. J., D. L. Brakensiek, and K. E. Saxton. 1982. “Estimation of Soil Water Properties.” *Transactions of the ASAE*, 25: 1316–1320 & 1328.

Rossman, L. A. 2015. “Storm Water Management Model User’s Manual Version 5.1.” 353.

Rossman, L. A., and J. T. Bernagros. 2019. *National Stormwater Calculatoir Web App User's Guide - Version 3.2.0*.

Sage, J., E. Berthier, and M.-C. Gromaire. 2015a. "Stormwater Management Criteria for On-Site Pollution Control: A Comparative Assessment of International Practices." *Environmental Management*, 56 (1): 66–80. https://doi.org/10.1007/s00267-015-0485-1.

Sage, J., E. Berthier, and M.-C. Gromaire. 2020. "Modeling Soil Moisture Redistribution and Infiltration Dynamics in Urban Drainage Systems." *Journal of Hydrologic Engineering*, 25 (9): 04020041. American Society of Civil Engineers. https://doi.org/10.1061/(ASCE)HE.1943-5584.0001978.

Sage, J., C. Bonhomme, S. Al Ali, and M.-C. Gromaire. 2015b. "Performance assessment of a commonly used 'accumulation and wash-off' model from long-term continuous road runoff turbidity measurements." *Water Research*, 78: 47–59. https://doi.org/10.1016/j.watres.2015.03.030.

Sage, J., E. El Oreibi, M. Saad, and M. C. Gromaire. 2016. "Modeling the temporal variability of zinc concentrations in zinc roof runoff-experimental study and uncertainty analysis." *Environmental Science and Pollution Research*, 23 (16): 16552–16566. Springer Verlag. https://doi.org/10.1007/s11356-016-6827-6.

Saltelli, A., P. Annoni, I. Azzini, F. Campolongo, M. Ratto, and S. Tarantola. 2010. "Variance based sensitivity analysis of model output. Design and estimator for the total sensitivity index." *Computer Physics Communications*, 181 (2): 259–270. https://doi.org/10.1016/j.cpc.2009.09.018.

Shojaeizadeh, A., M. Geza, J. McCray, and T. S. Hogue. 2019. "Site-Scale Integrated Decision Support Tool (i-DSTss) for Stormwater Management." *Water*, 11 (10). https://doi.org/10.3390/w11102022.

Traver, R. G., and A. Ebrahimian. 2017. "Dynamic design of green stormwater infrastructure." *Frontiers of Environmental Science & Engineering*, 11 (4): 15. https://doi.org/10.1007/s11783-017-0973-z.

Tuomela, C., N. Sillanpää, and H. Koivusalo. 2019. "Assessment of stormwater pollutant loads and source area contributions with storm water management model (SWMM)." *Journal of Environmental Management*, 233: 719–727. https://doi.org/10.1016/j.jenvman.2018.12.061.

US-EPA. 2016. *Summary of State Stormwater Standards*. 148. Environmental Protection Agency, Office of water.

Wang, J. 2019. "Development of Analytical Stochastic Models for Hydrologic Design of Stormwater Control Measures." PhD Thesis. McMaster University.

Zhang, K., and T. F. M. Chui. 2019. "Linking hydrological and bioecological benefits of green infrastructures across spatial scales – A literature review." *Science of The Total Environment*, 646: 1219–1231. https://doi.org/10.1016/j.scitotenv.2018.07.355.